DSM control strategy of solid oxide fuel cell distributed generation system

Junsheng Jiao*

School of Electrical Engineering, Tongling University, Tongling City, Anhui Province, China, 244061

Received 6 October 2013, www.tsi.lv

Abstract

The distributed power generation system of fuel cell has received the widespread attention in recent years for its pro-environment and high efficiency. The solid oxide fuel cell (SOFC) is a new power system, which turns chemical energy of fuels into electrical energy directly at middle and high temperature. Mathematical model of SOFC is analysed and the main circuit structure of independent power generation system is designed in this paper. The traditional PI control is adopted in DC/DC boost circuit to ensure the fuel cell can provide a stable DC output voltage. The three-phase inverter is used in DC/AC circuit and the dynamic equation derived from three-phase inverter is transformed to the synchronous rotating coordinate system. An innovative discrete sliding mode (DSM) control technology is applied and the system output stable sinusoidal AC voltage. The simulation experiments prove that SOFC power systems, in a certain range, can quickly and dynamically trace the change of the input voltage and load using DSM control.

Keywords: SOFC, Discrete Sliding Mode, Control, DC/AC, Converter

1 Introduction

As the global conventional energy is drying up and the environmental pollution problems are increasingly more serious, the distributed generation, in the form of small scale, scattered layout near the users and output the power independently, has received extensive attention for its advantages of pro-environment, high efficiency and flexible usage [1-2]. It will be an important part of micro grid in the future and a kind of competitive power in future power market.

Among various kinds of distributed generation system, fuel cell, wind, water, solar and other renewable energy have received great attention. The fuel cell is not like the wind and hydropower limited by geographical factors. It has a constant power output and advantages of high energy conversion efficiency, clean, no pollution and low noise [3-4]. It is suitable for either centralized power supply or distributed power supply and it also can be used as power supply of space vehicle, transportation. So it possesses more special application value.

Solid oxide fuel cell (SOFC) belongs to the third generation of fuel cell technology, the integrated thermoelectric efficiency of independent SOFC power system is 46% when the output power is 109KW [5-8]. It has the advantages of wide fuel adaptability, no leakage, high efficiency of comprehensive utilization and long service life. Therefore, it arouses people attention and is a hot and key point in the research of fuel cell. SOFC can be used as distributed power of network for fixed power generation. It also can provide mobile power supply for transportation tools, such as ships, vehicles, etc. [9-11]. Therefore, it is significant to develop the SOFC technology for improving the energy structure and maximizing the use of the existing energy and rare earth resources.

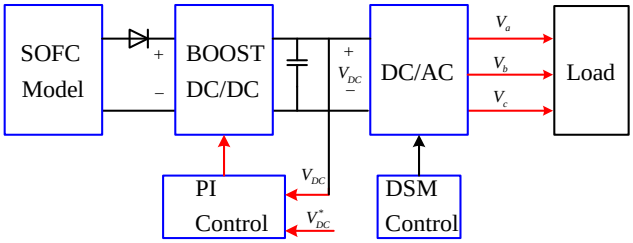

FIGURE 1 Main circuit of SOFC generation

Due to the output power of fuel cell is limited by its physical properties, when the load is changes, the response speed is slow. The SOFC power generation system designed in this paper uses DC/DC power converter to provide stable DC voltage for the use of three-phase DC/AC power converter and the discrete sliding mode control is used in DC/AC circuit. The simulation experimental results show that, with the support of the power electronic converter equipment, SOFC can provide stable power output for the network and fast load tracking capability.

* Corresponding author - Tel: +86-0562-588-2089 fax: +86-0562-588-2089;
E-mail: jiaotlu@sina.com

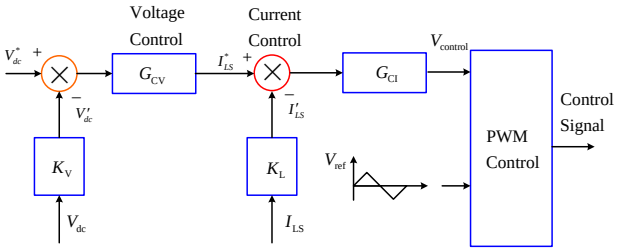

FIGURE 2 DC/DC PI control

2 SOFC model

The basic electrode reaction in the SOFC is different from that of other kinds of fuel cell [12]. The reaction is explained by the following formula:

$$\text{Anode: } H_2 + O^{2-} \rightarrow H_2O + 2e^-, \tag{1}$$

$$\text{Cathode: } \frac{1}{2}O_2 + 2e^- \rightarrow O^{2-}. \tag{2}$$

At the anode, hydrogen gas reacts with ions to create water in gaseous state and electrical energy is discharged in the configuration of the electrons. At the cathode, oxygen reacts with the electrons taken from the electrode, and oxygen ion is engendered. To count the open-circuit electromotive force of a stack of fuel cells in series, refer to the well-known Nernst formula [12]. In the formula above, E can be calculated by Nernst equation:

$$E = N_0 E_0 + E_f \ln\left(\frac{p_{H_2} p_{O_2}^{0.5}}{p_{H_2O}}\right), \tag{3}$$

where E_0 is the voltage associated with the reaction-free energy of a cell, $E_f = N_0 RT/2F$, R is the gas constant (8.31J/mol.K), T is the SOFC operating temperature, F is the Faraday constant (96487C/mol), and p_i are the partial pressures of hydrogen, oxygen and water.

3 Main circuit structure

Electrical energy from the fuel cell itself is usually not stable and the output voltage tends to be weak, it cannot use directly for load or electrical power grid. In order to meet the load demand, some corresponding converter devices is required. Main circuit of SOFC generation is in Figure 1. The first stage is usually DC/DC processing circuit. The converter turns the unstable output voltage of fuel cell into input voltage V_{DC} of the back stage inverter DC bus. The second stage is the inverter control, it is a core part of the distributed generation system, the current hot research spot and the technical difficulties are mainly concentrated in this part. The output DC voltage of SOFC boosts 35V by the boost converter; then three-phase AC sine voltage for load can be obtained from three-phase DC/AC inverter; after LC filter circuit 220V/50Hz AC output voltage is obtained.

4 DC/DC converter control

DC/DC boost converter control chart is exposed in Figure 2, V^*_{DC} is set as the boost instruction voltage. If the voltage is not reach the set value, the required current command produced by the voltage controller G_{CV} is compared with actual inductance current of converter, then the control command signal generated by the current controller is compared with the triangle wave to produce pulse width modulation signal, the duty ratio of the power switch is adjusted by control signals, the goal is to change the output voltage and achieve the stable output voltage.

The traditional PI control is illustrated in Figure 2. According to the classic laws of Ziegler -Nichols, V_{DC} is 35V. K_V of the inner current loop controller in DC/DC converter can be obtained as 19.72. In outer circle control loop, that is the voltage control loop and K_L is 82.36.

5 Three-phase DC/AC converter

Three-phase and three-leg DC/AC power converter, the structure is illustrated in Figure 3. DC shunt capacitance on the side stabilizes the output voltage. Three-phase voltage is generated by the on-off of control switch. Three legs and six switch components can be seen in Figure 3, two switches constitute a leg, each leg consists of two power switch element and their states of connection or break are complementary. That is when the upper leg switch VT_1, VT_3 and VT_5 are on, the lower leg switch VT_4, VT_6 and VT_2 are off, and vice versa. If the upper leg switch and lower leg switch of the same leg turn on, it will cause instantaneous short circuit and produce large current to burn down switch components.

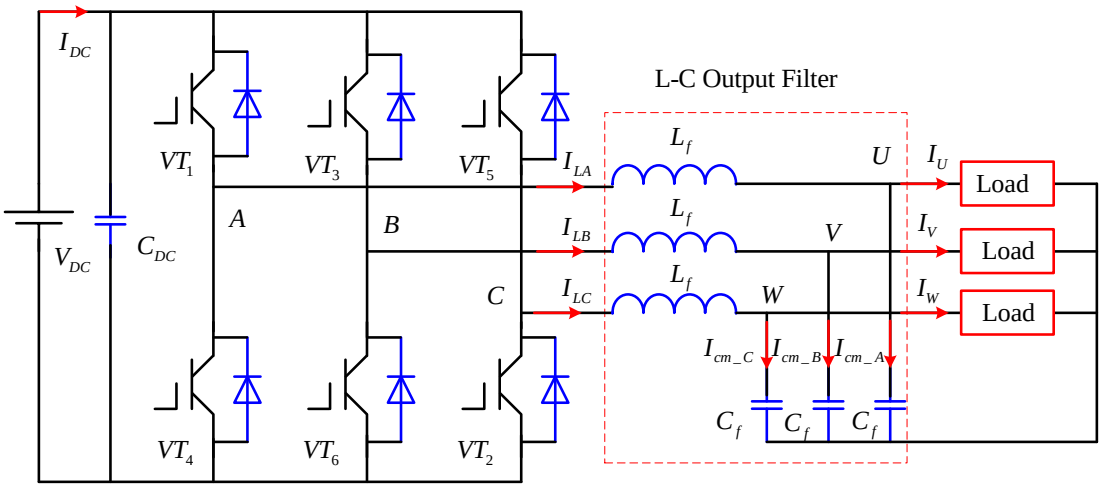

FIGURE 3 Three-phase DC/AC circuit

The circuit model explained by Figure 3 makes use of the following quantities [13]. The inverter output line-to-line voltage is expressed as the vector $V_i=[V_{iAB}\ V_{iBC}\ V_{iCA}]^T$, and the three-phase inverter output currents are I_{LA}, I_{LB} and I_{LC}. According as these currents, a vector is defined as $I_i=[I_{iAB}\ I_{iBC}\ I_{iCA}]^T=[I_{iA}\text{-}I_{iB}\ I_{iB}\text{-}I_{iC}\ I_{iC}\text{-}I_{iA}]^T$. Also, the line to line load voltage and phase load current vectors can he represented by $V_L=[V_{LAB}\ V_{LBC}\ V_{LCA}]^T$ and $I_L=[I_{LA}\ I_{LB}\ I_{LC}]^T$ respectively. On the L-C output filter, the following current and voltage equations are obtained after elementary calculation.

Voltage equations:

$$\begin{cases} \dfrac{dV_{LAB}}{dt}=\dfrac{1}{3C_f}I_{iAB}-\dfrac{1}{3C_f}(I_{LA}-I_{LB}) \\ \dfrac{dV_{LBC}}{dt}=\dfrac{1}{3C_f}I_{iBC}-\dfrac{1}{3C_f}(I_{LB}-I_{LC}) \\ \dfrac{dV_{LCA}}{dt}=\dfrac{1}{3C_f}I_{iCA}-\dfrac{1}{3C_f}(I_{LC}-I_{LA}) \end{cases}. \tag{4}$$

Current equations:

$$\begin{cases} \dfrac{dI_{iAB}}{dt}=-\dfrac{1}{L_f}V_{LAB}+\dfrac{1}{L_f}V_{iAB} \\ \dfrac{dI_{iBC}}{dt}=-\dfrac{1}{L_f}V_{LBC}+\dfrac{1}{L_f}V_{iBC} \\ \dfrac{dI_{iCA}}{dt}=-\dfrac{1}{L_f}V_{LCA}+\dfrac{1}{L_f}V_{iCA} \end{cases}. \tag{5}$$

Rewrite equation (4) and equation (5) into a vector form, respectively:

$$\begin{cases} \dfrac{dV_L}{dt}=\dfrac{1}{3C_f}I_i-\dfrac{1}{3C_f}T_iI_L \\ \dfrac{dI_i}{dt}=-\dfrac{1}{L_f}V_L+\dfrac{1}{L_f}V_i \end{cases}, \tag{6}$$

where $T_i=\begin{bmatrix} 1 & -1 & 0 \\ 0 & 1 & -1 \\ -1 & 0 & 1 \end{bmatrix}$.

6 Synchronous rotating transformation

The influence of mutual coupling and time-varying exists in the dynamic equations of three-phase coordinate system and the design of the controller will be more complex.

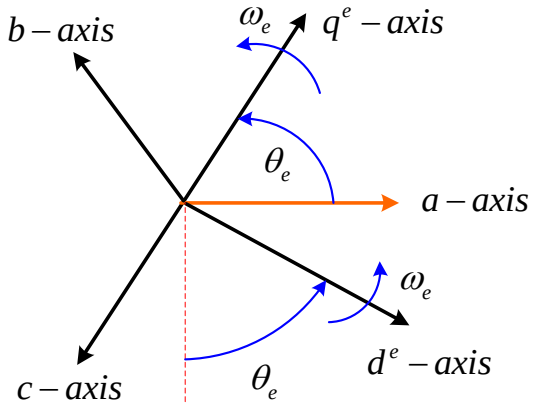

FIGURE 4 Synchronous rotating coordinate transformation

The derived dynamic equations can be converted into the synchronous rotating coordinate system before the design of controller. The geometric relations between three-phase coordinate system and the synchronous rotating coordinate system are shown as Figure 4.

The conversion relation is:

$$\begin{bmatrix} f_q^e \\ f_d^e \\ f_0^e \end{bmatrix} = T_{qd0}^e \begin{bmatrix} f_a \\ f_b \\ f_c \end{bmatrix} = \frac{2}{3} \begin{bmatrix} \cos\theta_e & \cos(\theta_e - \frac{2\pi}{3}) & \cos(\theta_e + \frac{2\pi}{3}) \\ \sin\theta_e & \sin(\theta_e - \frac{2\pi}{3}) & \sin(\theta_e + \frac{2\pi}{3}) \\ \frac{1}{2} & \frac{1}{2} & \frac{1}{2} \end{bmatrix} \begin{bmatrix} f_a \\ f_b \\ f_c \end{bmatrix}. \quad (7)$$

The inverse transform of the equation (7) is:

$$\begin{bmatrix} f_a \\ f_b \\ f_c \end{bmatrix} = \left[T_{qd0}^e\right]^{-1} \begin{bmatrix} f_q^e \\ f_d^e \\ f_0^e \end{bmatrix} = \begin{bmatrix} \cos\theta_e & \sin\theta_e & 1 \\ \cos(\theta_e - \frac{2\pi}{3}) & \sin(\theta_e - \frac{2\pi}{3}) & 1 \\ \cos(\theta_e + \frac{2\pi}{3}) & \cos(\theta_e + \frac{2\pi}{3}) & 1 \end{bmatrix} \begin{bmatrix} f_q^e \\ f_d^e \\ f_0^e \end{bmatrix}, \quad (8)$$

where f denotes either a voltage or a current variable; $\theta_e = \int 2\pi f_e dt$; f_e=50Hz.

Coordinating the transformation formula, the equation (4) and equation (5) are converted into the voltage and current equation of quadrature axis and direct axis in synchronous rotating coordinates, as shown in the equation (9) and equation (10) [14-15].

$$\begin{bmatrix} \frac{d}{dt} V_{q\_UVM}^e \\ \frac{d}{dt} V_{d\_UVM}^e \end{bmatrix} = \begin{bmatrix} 0 & -\omega_e \\ \omega_e & 0 \end{bmatrix} \begin{bmatrix} V_{q\_UVM}^e \\ V_{d\_UVM}^e \end{bmatrix} + \begin{bmatrix} \frac{1}{C_f} & 0 \\ 0 & \frac{1}{C_f} \end{bmatrix} \begin{bmatrix} I_{q\_abc}^e \\ I_{d\_abc}^e \end{bmatrix} + \begin{bmatrix} -\frac{1}{C_f} & 0 \\ 0 & -\frac{1}{C_f} \end{bmatrix} \begin{bmatrix} I_{q\_UVM}^e \\ I_{d\_UVM}^e \end{bmatrix}, \quad (9)$$

$$\begin{bmatrix} \frac{d}{dt} I_{q\_UVM}^e \\ \frac{d}{dt} I_{d\_UVM}^e \end{bmatrix} = \begin{bmatrix} 0 & -\omega_e \\ \omega_e & 0 \end{bmatrix} \begin{bmatrix} I_{q\_abc}^e \\ I_{d\_abc}^e \end{bmatrix} + \begin{bmatrix} \frac{1}{L_f} & 0 \\ 0 & \frac{1}{L_f} \end{bmatrix} \begin{bmatrix} V_{q\_abc}^e \\ V_{d\_abc}^e \end{bmatrix} + \begin{bmatrix} -\frac{1}{L_f} & 0 \\ 0 & -\frac{1}{L_f} \end{bmatrix} \begin{bmatrix} V_{q\_UVM}^e \\ V_{d\_UVM}^e \end{bmatrix}, \quad (10)$$

where $V_{q\_abc}^e$, $V_{d\_abc}^e$ is the output voltage of quadrature axis and direct axis for three phase DC/AC inverter respectively; $V_{q\_UVM}^e$, $V_{d\_UVM}^e$ is load voltage of quadrature axis and direct axis for three phase DC/AC inverter respectively; $I_{q\_abc}^e$, $I_{d\_abc}^e$ is the output current of quadrature axis and direct axis for three phase DC/AC inverter respectively; $I_{q\_UVM}^e$, $I_{d\_UVM}^e$ is the load current of quadrature axis and direct axis for three phase DC/AC inverter respectively.

7 Discrete sliding mode control

The design of discrete sliding mode controller includes two aspects [16]: one is to seek the sliding mode plane function, which makes the system sliding mode motion on the surface stable gradually and has good quality. The second is the designing of variable structure control, which can make the system reach the sliding surface from any point of phase space in finite time and form sliding mode control at sliding surface.

The continuous-time state space equation (9) and equation (10) of the plant system can be expressed to include dynamics of DSM below:

$$\begin{cases} \dot{X}(t) = AX(t) + Bu(t) + Ed(t) \\ y(t) = CX(t) \end{cases}, \quad (11)$$

where $X(t)$ is the system state vector, $X(t) \in R^n$; $u(t)$ is the system control vector, $u(t) \in R^m$; $d(t)$ is the system matching noise, $d(t) \in R^m$.

Given the sampling period T_z, the equation (11) can be transformed to the following discrete-time state space equation:

$$\begin{cases} X(k+1) = A^* X(k) + B^* u(k) + E^* d(k) \\ y(k) = CX(k) \end{cases}, \quad (12)$$

where $A^* = e^{AT_z}$, $B^* = \int_0^{T_z} e^{A(T_z - \tau)} B d\tau$, $E^* = \int_0^{T_z} e^{A(T_z - \tau)} E d\tau$.

In order to control the output $y(k)$ to follow the reference $y_{ref}(k)$, a sliding mode manifold may is selected in the following.

$$s(k) = y(k) - y_{ref}(k) = CX(k) - y_{ref}(k), \tag{13}$$

where $y_{ref}(k) = I_{cmd\_iqd}(k)$.

In other words, when the discrete sliding mode exists, which means $s(k)=0$, the output $y(k)$ is identical to the reference $y_{ref}(k)$. Therefore, the discrete sliding mode exists if the control input $u(k)$ is designed as following:

$$\begin{aligned} &s(k+1) = y(k+1) - y_{ref}(k+1) \\ &= CA^* X(k) + CB^* u(k) + CE^* d(k) - y_{ref}(k+1) = 0 \end{aligned} \tag{14}$$

The control algorithm that satisfies equation (14) and yields motion in the manifold $s(k)=0$ is called equivalent control. For the given system, the equivalent control $u_{eq}(k)$ is given as follows:

$$u_{eq}(k) = (CB^*)^{-1}\left[y_{ref}(k+1) - CA^* X(k) - CE^* d(k)\right] \tag{15}$$

Then the required control command can be calculated.

Discrete slide model control is based on the double loop control of voltage and current and turns the voltage equation (9) into the discrete state equation [17-18].

$$\begin{aligned} \begin{bmatrix} V^e_{q\_UVW}(k+1) \\ V^e_{d\_UVW}(k+1) \end{bmatrix} &= A_1^* \begin{bmatrix} V^e_{q\_UVW}(k) \\ V^e_{d\_UVW}(k) \end{bmatrix} + B_1^* \begin{bmatrix} i^e_{q\_abc}(k) \\ i^e_{d\_abc}(k) \end{bmatrix} \\ &+ D_1^* \begin{bmatrix} i^e_{q\_UVW}(k) \\ i^e_{d\_UVW}(k) \end{bmatrix} \end{aligned}, \tag{16}$$

where $A_1^* = \begin{bmatrix} 0 & -\omega_e \\ \omega_e & 0 \end{bmatrix}$, $B_1^* = \begin{bmatrix} \frac{1}{C_f} & 0 \\ 0 & \frac{1}{C_f} \end{bmatrix}$,

$D_1^* = \begin{bmatrix} -\frac{1}{C_f} & 0 \\ 0 & -\frac{1}{C_f} \end{bmatrix}$.

The feedback values of three-phase voltage and current are substituted into the equation (17) through synchronous rotating coordinate conversion. The filtering inductance current command $i^*_{q\_abc\_cmd}$, $i^*_{d\_abc\_cmd}$ can be acquired.

$$\begin{aligned} &\begin{bmatrix} i^e_{q\_abc\_cmd} \\ i^e_{d\_abc\_cmd} \end{bmatrix} = \\ &B'\left\{\begin{bmatrix} V^e_{q\_UVW} \\ V^e_{d\_UVW} \end{bmatrix} - A_1' \begin{bmatrix} V^e_{q\_UVW} \\ V^e_{d\_UVW} \end{bmatrix} - D_1' \begin{bmatrix} i^e_{q\_UVW} \\ i^e_{d\_UVW} \end{bmatrix}\right\}, \end{aligned} \tag{17}$$

where $A_1' = \begin{bmatrix} 1 & 0 \\ 0 & 1 \end{bmatrix} A_1^*$, $B_1' = \left\{\begin{bmatrix} 1 & 0 \\ 0 & 1 \end{bmatrix} B_1^*\right\}^{-1}$,

$D_1' = \begin{bmatrix} 1 & 0 \\ 0 & 1 \end{bmatrix} D_1^*$.

The current loop equation (10) can be converted into discrete state equations.

$$\begin{aligned} \begin{bmatrix} i^e_{q\_abc}(k+1) \\ i^e_{d\_abc}(k+1) \end{bmatrix} &= A_2^* \begin{bmatrix} i^e_{q\_abc}(k) \\ i^e_{d\_abc}(k) \end{bmatrix} \\ &+ B_2^* \begin{bmatrix} V^e_{q\_abc}(k) \\ V^e_{d\_abc}(k) \end{bmatrix} + D_2^* \begin{bmatrix} V^e_{q\_UVW}(k) \\ V^e_{d\_UVW}(k) \end{bmatrix} \end{aligned}, \tag{18}$$

where $A_2^* = \begin{bmatrix} 0 & -\omega_e \\ \omega_e & 0 \end{bmatrix}$, $B_2^* = \begin{bmatrix} \frac{1}{L_f} & 0 \\ 0 & \frac{1}{L_f} \end{bmatrix}$,

$D_2^* = \begin{bmatrix} -\frac{1}{L_f} & 0 \\ 0 & -\frac{1}{L_f} \end{bmatrix}$.

Taking the filtering inductance current commands and three-phase voltage obtained by synchronous rotating coordinate transformation into equation (19), the output voltage adjustment of three-phase DC/AC converter can be obtained.

$$\begin{aligned} &\begin{bmatrix} V^e_{q\_abc\_cmd} \\ V^e_{d\_abc\_cmd} \end{bmatrix} = \\ &B_2'\left\{\begin{bmatrix} I^e_{q\_abc} \\ I^e_{d\_abc} \end{bmatrix} - A_2' \begin{bmatrix} I^e_{q\_abc} \\ I^e_{d\_abc} \end{bmatrix} - D_2' \begin{bmatrix} V^e_{q\_UVW} \\ V^e_{d\_UVW} \end{bmatrix}\right\}, \end{aligned} \tag{19}$$

where $A_2' = \begin{bmatrix} 1 & 0 \\ 0 & 1 \end{bmatrix} A_2^*$, $B_2' = \left\{\begin{bmatrix} 1 & 0 \\ 0 & 1 \end{bmatrix} B_2^*\right\}^{-1}$,

$D_2' = \begin{bmatrix} 1 & 0 \\ 0 & 1 \end{bmatrix} D_2^*$.

8 Simulation results

The software of Matlab/Simulink is used for simulation analysis in the paper and Figure 5 shows the output voltage waveform of DC/DC converter. When the input voltage of SOFC drops down at t=0.1s, the change of the boost converter can be seen in Figure 5. As the decline of input voltage, the output voltage of boost converter drops down instantaneously. However, the output DC voltage can restore 35V at short time for the error compensation action of controller.

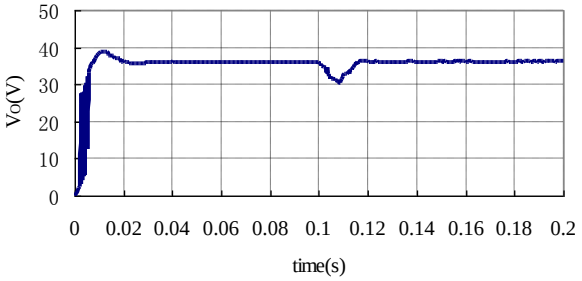

FIGURE 5 Output response of DC/DC

The independent operation mode is shown in Figure 6. The three-phase equilibrium resistive load, when the load power is 2000W, the output voltage and current of three-phase power converter are controlled by DSM controller. It can be seen from Figure 6, the peak value of output a phase voltage is about 311V and a peak value of phase current is about 4.28A.

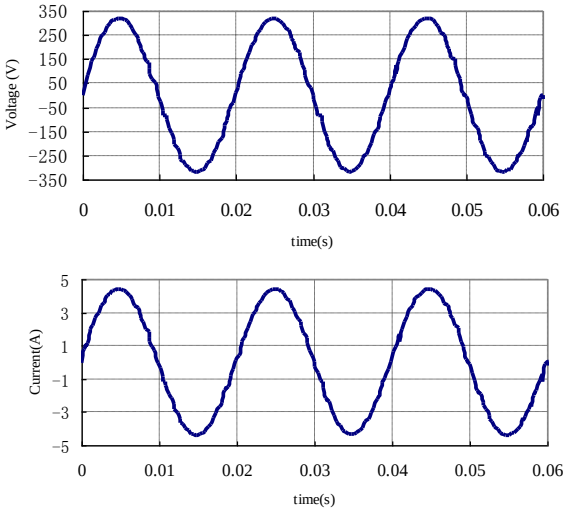

FIGURE 6 Output response of voltage and current of three-phase DC/AC inverter

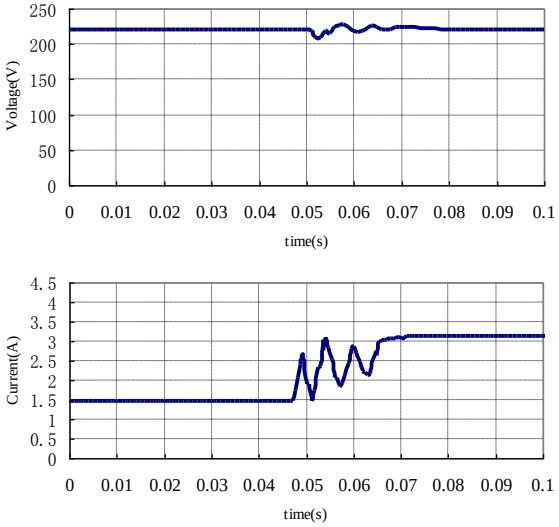

FIGURE 7 Output response of voltage and current RMS value for three-phase DC/AC inverter in load variation

When load is changed, Output response of voltage and current RMS value is shown in Figure 7 for three-phase DC/AC power converter. When it is increased from 990W to 2000W at 0.01s, the RMS (root mean square) value of voltage and current can be obtained. It is can be seen from Figure 7, which the voltage can restore stable in 0.015s by DSM controller, the current can restore stable in 0.023s.

9 Conclusion

The SOFC generation system based on PI and discrete slide mode control is designed in this paper. Its output power can reach 2000W and it can be applied in the SOFC generation system. When the load of three-phase power converter is changed, the voltage and current can be effectively controlled by DSM controller with fast dynamic response. The convergence rate is fast and there is no overshoot. The output of power is stable. It is more suitable for distributed generation system at steady state. The simulation results verify the feasibility of control algorithm.

References

[1] Sopian K, Wan Daud W 2006 Challenges and future developments in proton exchange membrane fuel cells *Renewable Energy* **31**(5) 719-27
[2] Olsen F A, Berenguer M G, Molina 2010 Design of improved fuel cell controller for distributed generation systems International *Journal of Hydrogen Energy* **35**(11) 5974-80
[3] Bauen A, Hart D, Chase A 2003 Fuel cells for distributed generation in developing countries-an analysis *International Journal of Hydrogen Energy* **28**(7) 695-701
[4] Vijay P, Samantaray A K, Mukherjee A 2009 A bond graph model-based evaluation of a control scheme to improve the dynamic performance of a solid oxide fuel cell *Mechatronics* **19**(4) 489-502
[5] Kaneko T, Brouwer J, Samuelsen G S 2006 Power and temperature control of fluctuating biomass gas fueled solid oxide fuel cell and

micro gas turbine hybrid system *Journal of Power Sources* **160**(1) 316-25
[6] Allag T, Das T 2012 Robust control of solid oxide fuel cell ultracapacitor hybrid system *IEEE Transactions on Control Systems Technology* **20**(1) 1-10
[7] Li Y H, Rajakaruna S, Choi S S 2007 Control of a solid oxide fuel cell power plant in a grid-connected system *IEEE Transactions on Energy Conversion* **22**(2) 405-13
[8] Komatsu Y, Kimijima S, Szmyd J S 2013 Numerical analysis on dynamic behavior of solid oxide fuel cell with power output control scheme *Journal of Power Sources* **233**(2) 232-45
[9] Caisheng Wang, Nehrir M H 2007 Short-time overloading capability and distributed generation applications of solid oxide fuel cells *IEEE Transactions on Energy Conversion* **22**(4) 898-906
[10] Du W, Wang H F, Zhang X F, Xiao L Y 2012 Effect of grid-connected solid oxide fuel cell power generation on power systems small-signal stability *IET Renewable Power Generation* **6**(1) 24-37
[11] Saha A K, Chowdhury S, Chowdhury S P, Song Y H 2007 Application of solid-oxide fuel cell in distributed power generation *IET Renewable Power Generation* **1**(4) 193-202
[12] Vikram M, Vinod M J, Steffen T, Olaf D 2012 A novel approach to model the transient behavior of solid-oxide fuel cell stacks *Journal of Power Sources* **214**(9) 227-38
[13] Ito Y, Kawauchi S 1995 Microprocessor based robust digital control for UPS with three-phase PWM inverter *IEEE Transactions on Power Electronics* **10**(2) 196-204
[14] Ilyas E 2006 Sliding mode control with PID sliding surface and experimental application to an electromechanical plant *ISA Transactions* **45**(1) 109-18
[15] Castaneda C E, Loukianov A G, Sanchez E N, Castillo-Toledo B 2012 Discrete-time neural sliding-node block control for a DC motor with controlled flux *IEEE Transactions on Industrial Electronics* **59**(2) 1194-1207
[16] Schirone L, Celani F, Macellari M 2012 Discrete-time control for DC-AC converters based on sliding mode design *IET Power Electronics* **5**(6) 833-40
[17] Hassan S, Seyyed M M K, Gholamreza V, Aria A 2009 Stabilizing unstable fixed points of discrete chaotic systems via quasi-sliding mode method *Communications in Nonlinear Science and Numerical Simulation* **14**(3) 839-49
[18] Utkin V, Guldner J, Shi J 1999 *Sliding Mode Control in Electromechanical Systems* CRC Press: Boca Raton

Authors

Junsheng Jiao, born in October, 1968, Wuwei County, Anhui Province, P.R. China

Current position, grades: the Associate Professor of School of Electrical Engineering, Tongling University, China.
University studies: received his B.Sc. in Electrical Engineering and Automation from Anhui University of Science and Technology in China. He received his M.Sc. from Jiangsu University in China.
Scientific interest: His research interest fields include power electronics, renewable energy and simulation.
Publications: more than 10 papers published in various journals.
Experience: He has teaching experience of eight years, has completed three scientific research projects.